Journal of Solid Mechanics Vol. 13, No. 3 (2021) pp. 338-348
DOI: 10.22034/jsm.2020.1897805.1580

Experimental and Numerical Investigation of the Impact of a Blunt Projectile with a Perforated Plate

M. Farahmand, Kh. Vahedi*, A. Naddaf Oskouei, R. Hoseini

Department of Mechanical Engineering , Imam Hossein Comprehensive University, Tehran, Iran

Received 20 June 2021; accepted 17 August 2021

ABSTRACT

This paper experimentally and numerically investigated the impact of a blunt projectile to perforated steel targets. In this study, projectiles were made of AISI 52100 and perforated plates were made of AISI 1045. In order to investigate the effect of the hole diameter on the projectile, three different diameters of the hole were considered, along with the effect of the projectile overlap with the hole. After examining different hitting states, the projectile was deviated from its movement direction after hitting the hole and changed from vertical hit to skew. The deviation of the projectile increased when the diameter of the hole increased or the amount of projectile overlap with the hole increased. Then, numerical modeling of impacting the projectile was performed by ABAQUS software and the results were compared with experimental results and the accuracy of the model was confirmed. And this model was used to investigate the effect of initial projectile speed on deviation of the projectile, accordingly, an increase in the initial velocity of the impact led to an increase in the deviation of the projectile.

Keywords: Target; Projectile deviation; Perforated plate; Impact; AISI 1045 Steel targets; AISI 52100 Steel Projectile.

1 INTRODUCTION

VARIOUS factors play a role in designing a suitable armor for a combat vehicle. The most important thing to keep in mind is that the armor should be effective in addition to being lightweight. One of the useful features of armor is related to its surface density, which is defined as the weight per square meter of the area perpendicular to the attack direction. In perforated plates, attempts are made to reduce the surface density of the armor while maintaining deterrence. Auyer [1] evaluated perforated metal armor with triangular holes. In this model, the armor is heated treatment to have a hard-outer surface and flexible inner surface. In this research, 2 armors have been used. The holes of the 2 perforated plates (holes of the outer and inner plates) are positioned so that they deviate from each other and prevent direct movement on the line of penetration of the projectile of any size. The ballistic armor with a high-strength steel plate as a secondary armor was invented by Ravid & Hirchberg [2]. In this study, the total area of the holes was between 40 and 50% of the total area of the armor. The distance from the center to the center of the holes was 1.2 to 1.9 times the diameter of the holes, which reduces the bullet damage of small caliber weapons. Balos et al.

*Corresponding author. Tel.: +98 2134521596.
E-mail address: Khvahedi@ihu.ac.ir (Kh.Vahedi)

[3] concluded that the optimally selected perforated plates can cause repeated fractures of projectile core up to 5 parts where the fragments are not able to penetrate the main plate, They observed that if we consider the ratio of the diameter of the hole to the distance between the two holes to be constant, decreasing the diameter of the hole also reduces the distance between the two holes and has less effect on the projectile, but on the other hand due to smaller hole diameter And the distance between the two holes will be less, the length of crack growth will be less and the damaged surface will be less. Madhu et al. [4] experimentally proved the positive effect of these armors and concluded that the performance of the ballistic armor against the 7.62 *mm* AP bullets improved by 2.4 times by adding perforated armor. Balos et al. [5] observed that the perforated plate with larger hole diameter is more effective in crushing the projectile core, and the perforated plates with a hole diameter similar to the diameter of the projectile core lead to earlier separation of the projectile, which are more effective in crushing the projectile. The hole edge has two opposite effects on the projectile. The first is caused by bending stress and causes the projectile to bend and fail. The second effect acts opposite to the first. It stabilizes the projectile, and the effect of the second factor becomes smaller and the projectile crushes more easily when the hole diameter increases. By considering the thickness of the perforated plate and its flexibility, a better and more beneficial effect is observed when a thicker plate is selected with a hard surface and a soft core [6]. Mishra [8] reported that the number of involved and connected holes decreases when the diameter of hole increases, Increasing the diameter of the holes has a positive effect on the effective mass and preservative properties of the mesh plate. Rosenberg [9] studied the breaking mechanism of the projectile by simulation and experimental testing and concluded that a high-strength oblique plate can break the projectile. Kilic and Bedir [10] demonstrated that the three effects of the perforated plate on the projectile include asymmetric axial force which deviates bullet path, bullet core fracture, and the erosion of the nose of bullet core, They observed that the projectile's nose eroded due to impact with the perforated plates, Or the core of the bullet splits into pieces and no sharp penetration is seen on the target plate.

Research on perforated targets has been very limited and the extent of projectile deviation after impact has not yet been investigated. And only the extent to which these targets are effective in defeating gun bullets has been studied. In this paper, the effect of the perforated plate on the deflection of the blunt projectile after impact is investigated experimentally and numerically. And after comparing the experimental and numerical results, the accuracy of the numerical model has been proved and then the numerical model has been developed by increasing the initial velocity of the projectile and its effect on the projectile deflection after hitting the perforated plate.

2 LABORATORY STUDIES

This section provides the components, used devices, and different tested modes in this research.

2.1 Target plate

The targets designed in this experiment are 10×100×120 *mm* and made of AISI 1045 steel. Three types of hole arrangements were applied to evaluate the effect of the diameter of the hole on projectile deviation.

- Holes with circle cross section and diameter of 5 *mm*
- Holes with circle cross section and diameter of 7 *mm*
- Holes with circle cross section and diameter of 9 *mm*

(a) (b) (c)

Fig.1
Types of perforation, a) 5*mm* diameter, b) 7*mm* diameter, c) 9*mm* diameter.

2.2 Projectile design

The used projectile in this experiment was a cylindrical roller bearing with a diameter of 10 *mm* and 20 *mm* length, made of AISI 52100 steel and weighing 12 grams.

Fig.2
The projectile used in this experiment.

2.3 Designing sabot

Sabot was used for this purpose since the caliber of the gas gun in the laboratory was 16 *mm* and the diameter of the projectile in the experimental tests was 10 *mm*. In order to make the sabot, a polymer rod with 20 *mm* diameter was divided into 20 *mm* pieces and then turned to have inner diameter 10 *mm* and 15.9 *mm* of outer diameter.

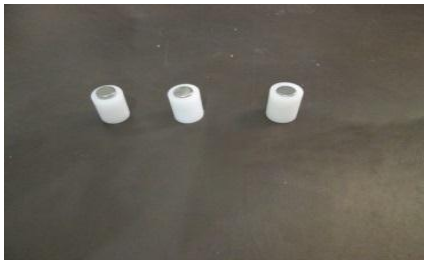

(a)

(b)

Fig.3
a) Built-in sabot (b) How the projectile is placed in the sabot.

2.4 Used equipment

In order to prevent the plate from moving after the hit of the projectile, the steel targets were fixed by a fixture as shown below.

Fig.4
Fixture used in this experiment.

A gas gun was used to launch the projectile. The gas gun applied in the hit laboratory is as follows:

Fig.5
Gas gun used in experiments.

The experiments were performed to investigate the effect of the hole on the projectile with an average velocity of 220 *m/s* through different diameters of hole and overlaps.

3 MODELING AND SIMULATING THE PROCESS

The initial energy of the bullet after hitting the steel plate is spent on deformation and heat release. Therefore, the temperature of the hit zone locally increases causing local smoothness of the metal in the hit zone. Therefore, the mechanical behavior of the steel plate is also temperature dependent. For this reason, Johnson-Cook equation was used to model the plastic behavior of the steel plate. The Johnson-Cook flow stress model is a visco-plastic model for soft materials. According to this model, strain hardening, strain hardening rate, and thermal softening have transient effect on the flow material stress.

$$\sigma_y\left(\varepsilon_p,\dot{\varepsilon}_p,T\right)=\left(A+B\left(\varepsilon_p\right)^n\right)\left(1+C\ln\left(\dot{\varepsilon}_p^*\right)\right)\left(1-T^{*m}\right) \tag{1}$$

In the above relation *A, B, C, n* and m are the constant properties of the material, $\dot{\varepsilon}_p$ is the equivalent plastic strain rate, $\dot{\varepsilon}_p^*$ represents the dimensionless plastic strain rate, and T^* is the normalized homogeneous temperature.

$$\dot{\varepsilon}_p^*=\frac{\dot{\varepsilon}_p}{\dot{\varepsilon}_0} \tag{2}$$

$$T^*=\frac{T-T_{initial}}{T_{melt}-T_{initial}} \tag{3}$$

Thus, we have:
Stress constants can be obtained as follows:

- ✓ *A* equal to the quasi-static yield stress
- ✓ *n* the slope value of σ-σ_{yield} curve in plastic strain
- ✓ *B* the value of σ-σ_{yield} in plastic strain equal to one
- ✓ *c* the slope of the stress curve in terms of the variable strain rate at room temperature
- ✓ $m=\log\left(1-\frac{\sigma}{\sigma_{room}}\right)$, where σ_{room} is a given stress at room temperature.

Among the above parameters, the values of *A, B* and *n* are obtained by static tensile test, which is why they are called quasi-static constants and their values are generally between 0.001-1. The *c* and m constants are determined by the torsion test at different strain rates and temperatures and the Hopkinson pressure bar test.
In this material model, the failure strain is expressed as follows:

$$\varepsilon^f=\left(D_1+D_2\exp D_3\sigma^*\right)\left(1+D_4\varepsilon^*\right)\left(1+D_5T^*\right) \tag{4}$$

The D_1 and D_2 and D_3 constants are stress-dependent, while the D_4 constant depends on the strain hardening rate and the D_5 constant relies on the softening temperature. σ^* is obtained by dividing the pressure by the effective stress.

According to this model, damage to the material accumulates during plastic strain and failure occurs when the sum of these values reaches a critical limit where failure coefficient D is equal to one.

$$D = \sum \frac{\Delta \varepsilon^{-P}}{\varepsilon^f} \tag{5}$$

3.1 Boundary and basic conditions

In all simulations, the boundary conditions are defined as the lateral edges of the target are bound at all six degrees of freedom, but there is no movement constraint for the projectile to move in different directions.

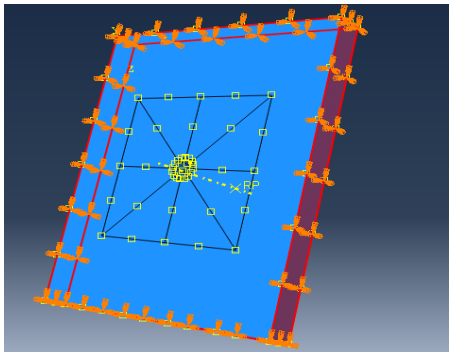

Fig.6
The side edges of the target are bound at every six degrees of freedom.

The velocity of projectile is 220 *m/s* and the initial temperature of the target plate is $27^{\circ}C$. The contact between the projectile and the plate is in the form of general contact and the type of contact is tangential behavior with friction coefficient of 0.02 and normal behavior.

3.2 Specifications of projectile and target

The specifications of the AISI 1045 steel plates used in the tests are as follows:

Table 1
Properties of AISI 1045 steel plates [11].

Modulus of elasticity *GPa*	Poisson's Ratio	Density Kg/m^3	Thermal conductivity coefficient *Watt/m.K*	Linear expansion coefficient (10^{-6})	Special heat capacity *Watt/kg.K*
200	0.29	7870	51.9	11.2	486

The specifications of the AISI 52100 steel projectile used in the tests are as follows:

Table 2
Properties of AISI 52100 steel projectiles[12].

Modulus of elasticity *GPa*	Poisson's Ratio	Density Kg/m^3	Thermal conductivity coefficient *Watt/m.K*	Linear expansion coefficient (10^{-6})	Special heat capacity *Watt/kg.K*
210	0.3	7800	46.6	1.19	480

The consonants in Johnson-Cook model were used in simulations as follows:

Table 3
Constants of the Johnson Cook equation for AISI 52100 [12].

Constants of the Johnson Cook equation	AISI 52100
A (MPa)	2482
B (MPa)	1498
N	0.19
C	0.027
M	0.66
Tmelt $(^{\circ}C)$	1487
$\dot{\varepsilon}_0$	0.001

Table 4
Constants of the Johnson Cook equation for AISI 1045 [11].

Constants of the Johnson Cook equation	AISI 1045
A (MPa)	553
B (MPa)	600
N	0.234
C	0.0134
M	1
Tmelt $(^{\circ}C)$	1460
$\dot{\varepsilon}_0$	0.001

Table 5
The rupture constants of the Johnson-Cook equation [11].

The rupture constants of the Johnson-Cook equation	D_1	D_2	D_3	D_4	D_5
AISI1045	0.06	3.31	-1.96	0.0018	.58

3.3 Discretization of projectile

The selected mesh for the projectile is in a way that the circular cross section of the projectile is 1 *mm* in diameter and 2 *mm* in length.

3.4 Discretization of Perforated plate

In order to obtain more precise answers, the hole of target plate was separated by a square with sides of 60 *mm*, and then partitioned (to obtain a regular mesh) with finer meshes.

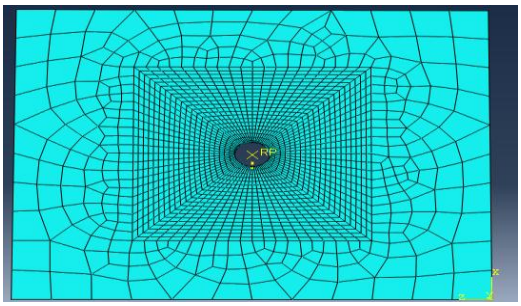

Fig.7
Mesh of Perforated plate.

4 RESULTS AND DISCUSSION

4.1 Experimental results

The method of obtaining exact location of projectile hit and the deviation from vertical position are as follows:

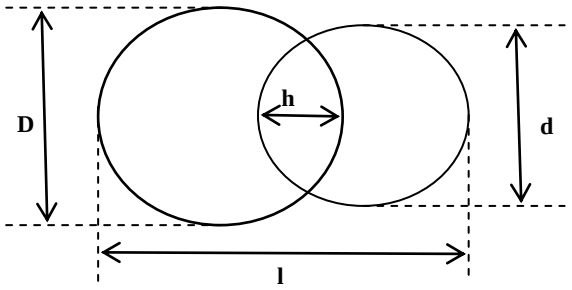

Fig.8
Introducing parameters and overlapping.

Overall length : l
The diameter of the hole : *d*
The length of an area of the projectile not involved with the hole : l-*d*
The length of projectile and hole contact area : *h*=*D*-(l-*d*)
The length of the area of the hole not in contact with the projectile : *d*-*h*
The minimum penetration depth of projectile (calculated by caliper) : y_{min}
The maximum penetration depth of projectile (calculated by caliper) : y_{max}
The amount of projectile deviation after hitting the hole:

$$\theta = \tan^{-1}\left\{\frac{y_{\max} - y_{\min}}{(1-d)}\right\} \tag{6}$$

4.1.1 The overlapping effect of the projectile with the hole

In order to evaluate the effect of the projectile overlap with the holes, the plates were considered with holes of 5 and 9 mm diameter and different overlapping rates. This section examines three hit modes for a plate with a diameter of 5 *mm* and two hit modes for a plate with a diameter of 9 *mm*.

The hole with 5 mm diameter and 1 mm overlap
l =14, d =5, y_{min} =0.9, y_{max} =1.7, $\theta = 5.07$

The hole with 5 mm diameter and 3 mm overlap
l =12, d =5, y_{min} =0.9, y_{max} =1.08, $\theta = 7.73$

The hole with 5 mm diameter and 4.2 mm overlap
l =10.8, d =5, y_{min} =1.1, y_{max} =2, $\theta = 8.82$

Fig.9
Perforated plate with 5 mm diameter hole and different overlap.

The hole with 9 *mm* diameter and 4 mm overlap
$l=15$, $d=9$, $y_{min}=1.2$, $y_{max}=2.3$, $\theta=10.38$

The hole with 9 *mm* diameter and 6 mm overlap
$l=13$, $d=9$, $y_{min}=1.7$, $y_{max}=2.5$, $\theta=11.3$

Fig.10
Perforated plate with 5 mm diameter hole and different overlap.

By examining the amount of overlap on a perforated plate with fixed diameter, the deviation of the projectile after hitting the target increases by increasing overlapping.

4.1.2 Examining the effect of the hole diameter

In order to study the effect of the hole diameter, a comparison was made between perforated plates with hole diameters of 5, 7 and 9 *mm*. Comparison between the diameter of 5 and 9 *mm* holes with 4 *mm* overlapping.

(a)

(b)

Fig.11
(a) 5 *mm* diameter hole and 4.2 *mm* overlap (b) 9 *mm* diameter hole and 4 *mm* overlap.

The deviation after hitting the plate for the 5 and 9 *mm* hole diameters shown in Fig. (10) are 8.82 and 10.38 degrees, respectively.

(a)

(b)

Fig.12
(a) 7 *mm* diameter hole and 6 *mm* overlap (b) 9 *mm* diameter hole and 6 *mm* overlap.

The deviation after hitting the plate for the 7 and 9 *mm* hole diameters shown in Fig. (11) are 9.92 and 11.30 degrees, respectively. The comparison between 5, 7 and 9 *mm* diameter holes.

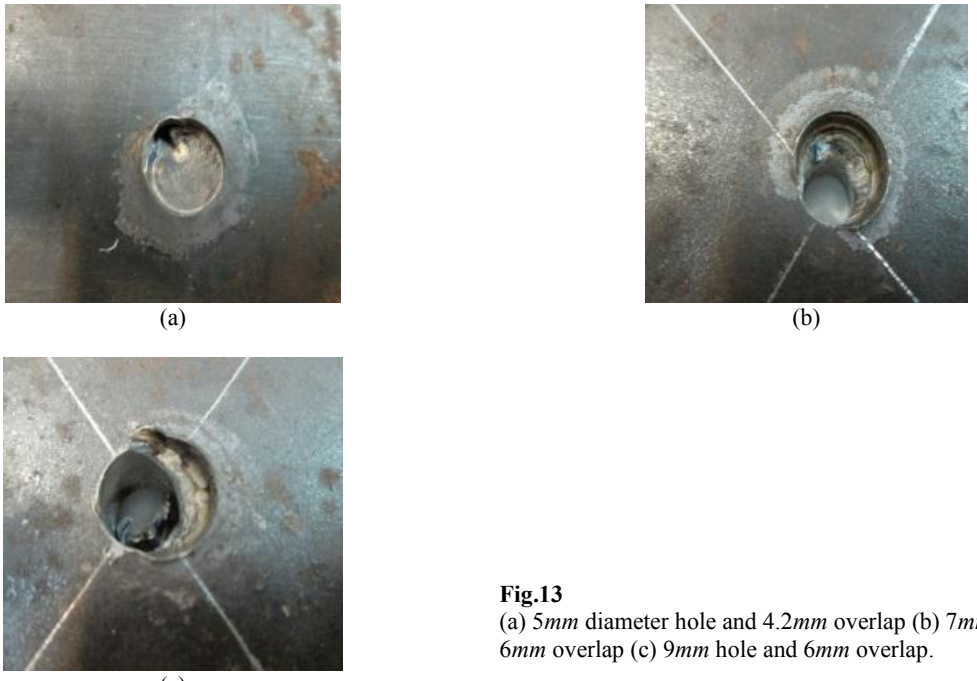

(a) (b) (c)

Fig.13
(a) 5*mm* diameter hole and 4.2*mm* overlap (b) 7*mm* hole and 6*mm* overlap (c) 9*mm* hole and 6*mm* overlap.

As it is observed in the figures, and according to the calculations of the previous section, the deviation rates after hitting the plate for the hole diameters of 5, 7, and 9 *mm* were obtained to be 8.82, 9.92, and 11.30 degrees, respectively. It can be claimed that the deviation of the projectile increases in the target plate by increasing the diameter of the hole. It is worth noting that the selected projectile has a very high strength and did not deform after hitting the target. Therefore, calculating the degree of deviation based on the changes made on the target surface indicates the exact amount of projectile deviation after hitting the target.

4.2 Numerical simulation

4.2.1 Calculating the penetration depth of the projectile after hitting the target in software

In simulation with the Query icon and selecting the distance from the popup menu, the height difference of two points can be observed in the simulation results section by selecting two points. This allows obtaining an accurate depth of penetration by selecting a point away from the hit point or selecting a point which are fixed at the boundary conditions as the first point and selecting another point where we are looking for projectile penetration value. In this section, the perforated plates with hole diameters of 5, 7 and 9 *mm* investigated in the previous section are simulated. Then, the differences between experimental and numerical values are evaluated.

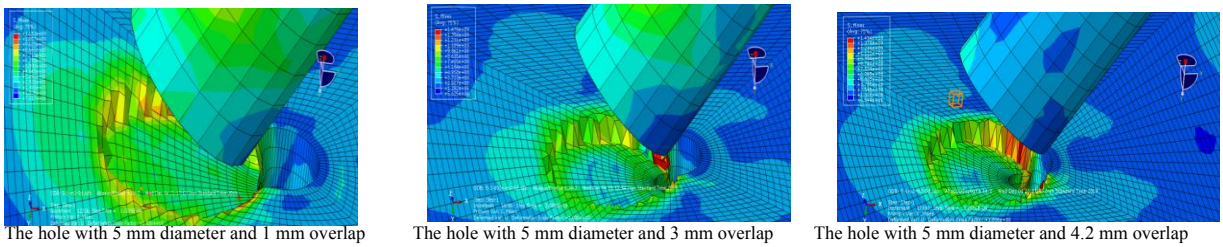

The hole with 5 mm diameter and 1 mm overlap
y_{min}=0.856, y_{max}=1.79, $\theta = 7.6$, error =4%

The hole with 5 mm diameter and 3 mm overlap
y_{min}=0.836, y_{max}=1.73, $\theta = 5.67$, error = 10%

The hole with 5 mm diameter and 4.2 mm overlap
y_{min}=0.911, y_{max}=1.76, $\theta = 8.05$, error =9%

Fig.14
Simulating the impact of projectile with a perforated plate of 5*mm* diameters.

Thus, we have:
y_{min} : Calculating the minimum penetration depth using the Query tool

y_{max} : Calculating the maximum penetration depth using the Query tool
θ : The deviation amount of the projectile after impacting the hole
error: Calculation of error in projectile deviation between numerical & experimental results

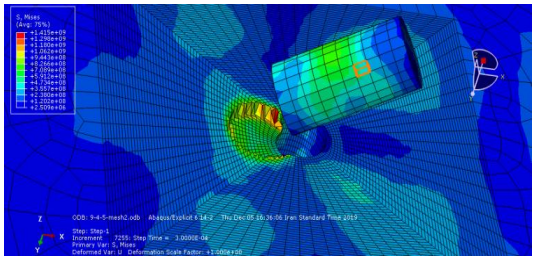

The hole with 9 *mm* diameter and 4 *mm* overlap
y_{min} =1.14, y_{max} =2.1, θ = 9.09 , error =12%

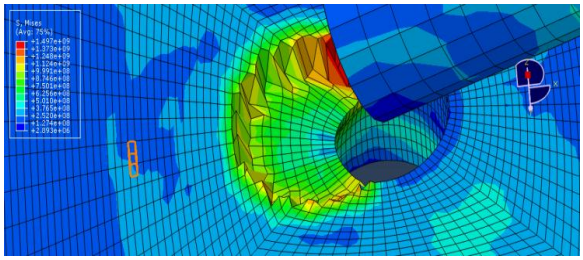

The hole with 9 *mm* diameter and 6 *mm* overlap
y_{min} =1.66, y_{max} =2.42, θ = 10.75 , error =5%

Fig.15
Simulating the impact of projectile with a perforated plate of 9*mm* diameters.

4.2.2 The effect of velocity of the projectile on its deviation

After proving the numerical model, the effect of the velocity of the projectile on the amount of projectile deviation after hitting the perforated surface was evaluated. In the first case, the perforated plate with 5 *mm* diameter and 2 *mm* overlap and initial velocities of 220, 280, 350, 420 and 500 were assessed and the deviation rates were obtained.

Table 6
Initial velocity & deviation for the hole diameter of 5 *mm* and 2 *mm* of overlapping.

Initial velocity	220	280	350	420	500
Deviation	6.58	8.11	10.2	12.9	15

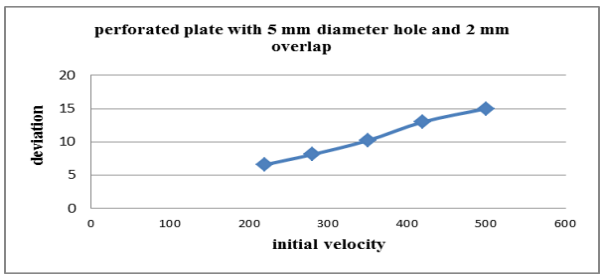

Fig.16
The deviation is obtained for the hole diameter of 5 *mm* and 2 *mm* of overlapping.

Then, the deviation is obtained for the hole diameter of 9 *mm* and 5 *mm* of overlapping.

Table 7
Initial velocity & deviation for the hole diameter of 9 *mm* and 5 *mm* of overlapping.

Initial velocity	220	280	350	420	500
Deviation	942.	13.92	18.1	21.2	24.5

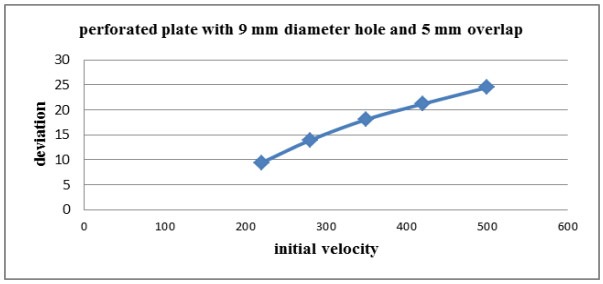

Fig.17
The deviation is obtained for the hole diameter of 9 *mm* and 5 *mm* of overlapping.

The deviation results of the projectile indicated that the deviation after hitting the perforated plate increases by increasing initial velocity.

5 CONCLUSIONS

1. In this paper, the experimental and numerical study of the impact of the blunt projectile on the perforated targets has been done.
2. The experimental tests of perforated plates were performed with three hole diameters of 5, 7 and 9 *mm* and average velocity of 220 *m/s*.
3. By examining the amount of overlap on a perforated plate with fixed diameter, the deviation of the projectile after hitting the target increases by increasing overlapping rate.
4. By evaluating the perforated plates with variable diameter and constant overlap, the deviation of the projectile increases after hitting the target when the hole diameter increases.
5. This paper discussed the numerical modeling of projectile penetration and the model was in good agreement with the experimental results.
6. After verifying the accuracy of numerical model, the effect of the impacting velocity of the projectile on the perforated plate was investigated. The results indicated that the deviation of the projectile increased through increasing initial velocity.
7. Therefore, perforated plates are effective in deflecting the direction of the projectile.
8. Perforated plates reduce structural mass and construction costs.

REFERENCES

[1] Auyer R.A., 1991, *Perforated Plate Armor*, Patent No: 5,014,593.
[2] Ravid M., Hirchberg Y., 2009, *Ballistic Armor*, Patent No: 7,513,186 B2.
[3] Balos S., Grabulov V. L., Sidjanin B., Pantic A., Radisavljevic I., 2010, Geometry, mechanical properties and mounting of perforated plates for ballistic application, *Materials and Design* **31**: 2916-2924.
[4] Madhu V., Bhat T.B., 2011, Armour protection and affordable protection for futuristic combat vehicles, *Defence Science Journal* **61**(4): 394-402.
[5] Ogorkiewitz R., 1991, *Technology of Tanks*, Coulsdon: Jane's Information Group Limited.
[6] Radisavljevic I., Balos S., Nikacevic M., Sidjanin L., 2013, Optimization of geometrical characteristics of perforated plates, *Materials and Design* **49**: 81-89.
[7] Chocron S., Anderson C.E., Grosch D.J., Popelar C.H., 2001, Impact of the 7.62-mm APM2 projectile against the edge of a metallic target, *International Journal of Impact Engineering* **25**: 423-437.
[8] Mishra B., Ramakrishna B., Jena P.K., Siva Kumar K., Madhu V., Gupta N.K., 2013, Experimental studies on the effect of size and shape of holes on damage and microstructure of high hardness armor steel plates under ballistic impact, *Materials and Design* **43**: 17-24.
[9] Rosenberg Z., Ashuach Y., Yeshurun Y., Dekel E., 2009, On the main mechanism for defeating AP projectiles, long rods and shaped charge jets, *International Journal of Impact Engineering* **36**: 588-596.
[10] Kilic N., Bedir S., Erdik A., Ekici B., Demirci A., Güden M., 2014, Ballistic behavior of high hardness perforated armor plates against 7.62 mm armor piercing projectile, *Materials and Design* **63**: 427-438.
[11] Duan C.Z., Dou T., Cai Y.J., Li Y.Y., 2011, Finite element simulation and experiment of chip formation process during high speed machining of AISI 1045 hardened steel, *Applied Mechanics and Materials* **29-32**: 1838-1843.
[12] Pawar S., Salve A., Chinchanikar S., Kulkarni A., Lamdhadeb G., 2017, Residual stresses during hard turning of AISI 52100 Steel: Numerical modeling with experimental validation, *5th International Conference of Materials Processing and Characterization*.